Environmental and human drivers of stony coral tissue loss disease (SCTLD) incidence within the Southeast Florida Coral Reef Ecosystem Conservation Area Final Report

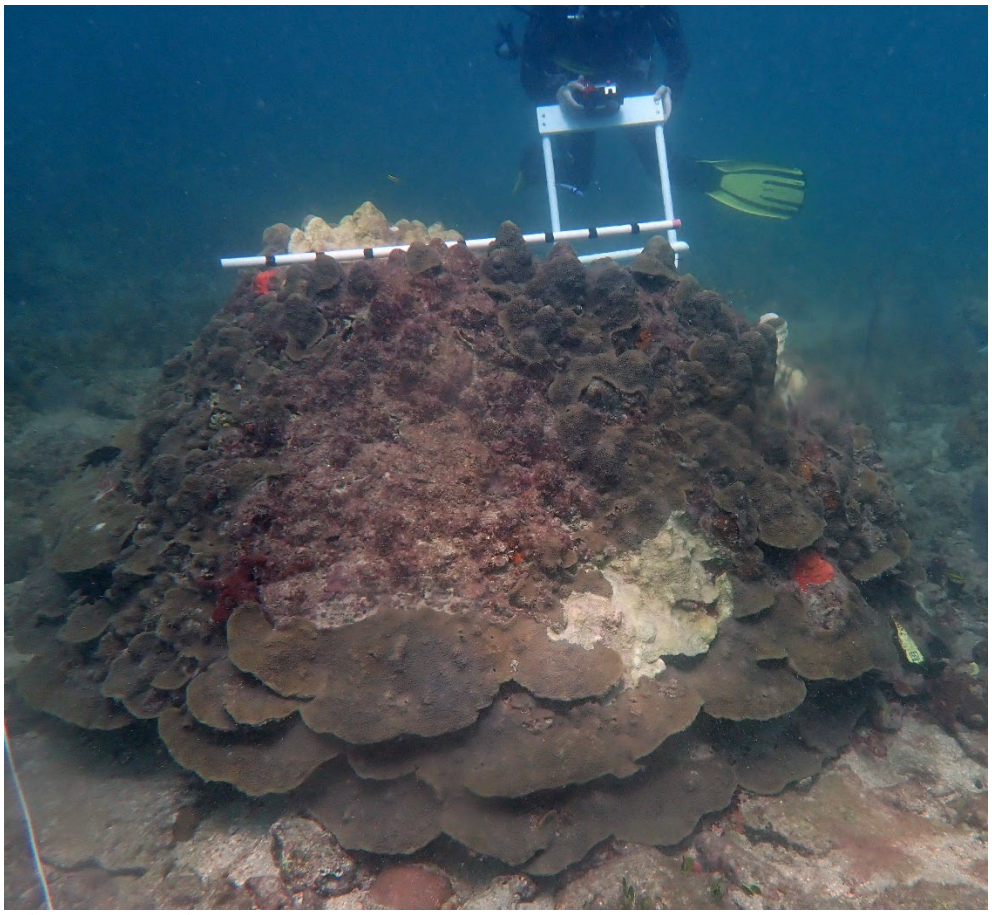

Colony LC-157 October 7, 2021

Report generated for:
Florida Department of Environmental Protection
Office of Resilience and Coastal Protection

Environmental and human drivers of stony coral tissue loss disease (SCTLD) incidence within the Southeast Florida Coral Reef Ecosystem Conservation Area
Final Report

Prepared By:

Brian K. Walker[1*], Gareth J. Williams[2*] Greta S. Aeby[3], Jeffrey A. Maynard[3], and David Whitall[4]

[1] Halmos College of Arts and Science, Nova Southeastern University, 8000 N. Ocean Drive, Dania Beach, FL 33004; walkerb@nova.edu, [2] School of Ocean Sciences, Bangor University, LL59 5AB, UK; g.j.williams@bangor.ac.uk, [3] SymbioSeas, 1114 Merchant Lane, Carolina Beach, NC, 28428, [4]NOAA NCCOS, Monitoring & Assessment Branch, Stressor Detection and Impacts Division, 1305 East-West Hwy, Silver Spring, MD 20910.

[*]*Contributed equally*

June 1, 2022

Completed in Fulfillment of PO B9CAF9 for

Florida Department of Environmental Protection
Office of Resilience and Coastal Protection
1277 N.E. 79th Street Causeway
Miami, FL 33138

This report should be cited as follows:
Walker BK, Williams GJ, Aeby GS, Maynard JA and Whitall D. 2022. Environmental and human drivers of stony coral tissue loss disease (SCTLD) incidence within the Southeast Florida Coral Reef Ecosystem Conservation Area, 2021-22. Final Report. Florida DEP. Miami, FL., XXX p.

This report was prepared for Nova Southeastern University. Funding was provided by the Florida Department of Environmental Protection Award No. B9CAF9. The views, statements, findings, conclusions and recommendations expressed herein are those of the authors and do not necessarily reflect the views of the State of Florida or any of its sub-agencies.

Table of Contents

List of Figures

List of Tables

1. EXECUTIVE SUMMARY

Designing intervention measures to reduce the impacts of coral disease on tropical coral reefs requires an understanding of the drivers of disease prevalence within coral populations. Oftentimes these are related to local or regional environmental stressors. If these drivers are tangible targets for management action, then decisions can be made to regulate the levels of these drivers and yield positive outcomes for the reef. This project combined *in situ* coral disease surveys, spatial data synthesis, and statistical modeling to identify the environmental and human drivers of Stony Coral Tissue Loss Disease (SCTLD) in the Kristin Jacobs Coral Reef Ecosystem Conservation Area (Coral ECA).

This report describes an effort to test whether there are predictable patterns of SCTLD incidence within a population of largest colonies being monitored monthly and treated when necessary. Several predictor variables hypothesized to be linked to SCTLD incidence were synthesized. These included abiotic environmental drivers (e.g., depth, seawater temperature, seawater nutrient concentrations) and human drivers (e.g., density of septic tanks as a proxy for human coastal development), outflow from the Inlet Contributing Areas (ICAs), and distance to offshore outfall locations). We calculated colony-specific estimates of these predictor variables and built statistical models to test their ability to explain spatial and temporal patterns in SCTLD infections.

The temporal model explained 56.4% of the temporal variation in the total number of SCTLD infections over time. SCTLD infections showed a positive correlation with temperature stress, inlet flow, and total rainfall. Outliers created high model error for both temperature stress and inlet flow towards the higher values of both predictors. It appears more SCTLD lesions develop over time following a pro-longed period of temperature stress, in particular when there has been over 150 'Hot Snap' exposure hours over the prior 90 days. This is then exacerbated by outflow from the ICA inlets and rainfall, in particular when there has been more than 5000 cubic feet per second summed flow coming out of the ICAs in the prior 7 days, and over 0.2 – 0.3 inches of rain per day in the prior 90 days.

The spatial model explained 38.0% of the spatial variation in the total number of SCTLD infections over the entire period. SCTLD infections showed a positive correlation with the number of septic tanks within a 5 km radius, with a noticeable increase in lesions occurring beyond ~100 tanks. The correlation with the distance to the Government Cut outfall was less clear, with the number of lesions maximized at mid-distances. This should be interpreted with caution, however, as the distance to Government Cut outfall highly correlated with the distance to both Hillsboro and Boca outfalls, suggesting that either of these distances might offer the same predictive power in the model.

These investigations showed that coastal urbanization and water management influence the number of coral disease lesions on Florida's Coral Reef within the Coral ECA. They suggest strong links between SCTLD infection levels and potential pollutants, or pathogens associated with the presence of anthropogenically impacted water flowing out of the inlets. The nature and extent of these links warrant urgent and immediate attention.

The sum consequence of the relationships identified herein is that global stressors on corals are being exacerbated by the local human impacts of runoff and land-based sources of pollution that elevate on-reef nutrient levels. Mitigating local stressors would make conditions for corals less conducive to disease. These links highlight that there are management, conservation, and stewardship actions in SE Florida that can increase reef resilience to climate change and disease outbreaks. For example, the timing of inlet outflow can be regulated to ensure high flow does not coincide with periods of high seawater temperature stress. Future work can help to shape and target this and a range of other actions to maximize our influence on the capacity of reefs in SE Florida to function and provide goods and services under climate change.

2. BACKGROUND

Spatial and temporal patterns of coral diseases on tropical reefs are often driven by a complex array of interacting environmental, anthropogenic and host-specific factors that affect both pathogen virulence and host resistance or susceptibility (Williams et al. 2010; Aeby et al. 2011b; Aeby et al. 2020). Given that the prevalence of diseases on reefs is expected to increase in the future (Maynard et al. 2015), identifying disease drivers is key to designing effective local mitigation strategies, prioritizing disease intervention resources, and identifying areas suitable for reef restoration. Identifying the drivers of coral disease dynamics requires detailed information on the spatial and temporal patterns of disease occurrence, characterization of the gradients in suspected drivers, and the combining of these data in a suitable statistical modeling framework (Williams et al. 2010).

Florida's Coral Reef is currently experiencing a multi-year coral disease mortality event from Stony Coral Tissue Loss Disease (SCTLD) that has resulted in extensive coral die-offs. Approximately 21 species of coral, including both Endangered Species Act-listed and the primary reef-builders, have displayed tissue loss lesions which often result in whole colony mortality. First observed near Virginia Key in late 2014, the disease has since spread to the northernmost extent of Florida's Coral Reef, and south to the Dry Tortugas (Muller et al. 2020). The best available information indicates that SCTLD is also spreading throughout the Caribbean (Alvarez-Filip et al. 2019; Estrada-Saldívar et al. 2021).

SCTLD's unique trait of affecting many species at varying infection and virulence rates remains perplexing. A number of species are known as highly susceptible because they typically get the disease first and are decimated quickly, while a second group are slower to infect and have slower lesion progression rates. In many cases, all or almost all of the susceptible species succumb to the disease leaving very few survivors. However, some persist. Recent recon efforts show a number of individuals of highly susceptible species (*Meandrina meandrites, Diploria labyrinthiformis*) in the endemic zone (Southeast Florida) begging the question: why did these individuals not succumb to the disease? Unfortunately, there are few survivors remaining and none of the more sensitive conspecifics are alive for comparisons.

The other less susceptible species (*Orbicella* spp.*, Montastraea cavernosa*) appear more resistant to infection because they can persist amongst other diseased corals for years before signs of infection. Once infection signs appear, lesions may rapidly kill a coral,

persist slowly for a long time, or in some cases disappear (apparently fought off by the coral holobiont). Understanding this dynamic requires knowledge of differing infection rates of individuals. This is difficult to ascertain without extensive monitoring and disease intervention because it will likely perish soon after becoming diseased if not treated. The disease intervention keeps the coral alive and the monitoring captures the timing of reinfections facilitating an understanding of the individual's susceptibility or resistance. Those that reside in the endemic zone alongside diseased colonies and yet have not been infected are assumed to be the most resistant.

Populations of Florida's mountainous star coral (*Orbicella faveolata*) are the subject of intensive disease intervention efforts to stop SCTLD. Successful disease intervention treatments on Florida's Coral Reef have kept diseased reef-building corals alive providing a unique opportunity to test intraspecific differences between groups of corals with differing infection patterns. Some corals get infected once, some are reinfected numerous times, and some not at all. Viewing this collection of *O. faveolata* as patients or individual cases that are grouped as at risk (no infection) or differentially affected (i.e., degrees of infection rates) by SCTLD, it is important to have a basic 'patient history' or anamnesis as a foundation to interpret and contextualize more probative or diagnostic analyses.

The intense successful disease intervention and monitoring provide an unprecedented *in situ* record of the occurrence of new SCTLD infections on a set of *O. faveolata* colonies. These data provide a measure of disease incidence and host susceptibility through time that can be related to concurrent spatial and temporal gradients in suspected drivers. This project builds upon previous efforts (Walker et al. 2021a) to identify the most influential drivers of SCTLD on *O. faveolata* corals within the Southeast Florida Coral Reef Ecosystem Conservation Area.

Project Goals and Objectives

This project builds upon previous data-driven statistical modelling efforts to capitalize on an additional 14 months of monitoring data for several monitored large corals in the Coral ECA collected from May 2020 to June 2021. These additional data increase the replication of the previous temporal model presented in Walker et al. (2021) from n=20 to n=34, therefore improving its statistical strength and importantly capturing another full seasonal cycle of SCTLD incidence (SCTLD incidence in the Coral ECA appears to peak in the summer months). If after adding these additional data there is once again a robust quantitative correlation between SCTLD incidence and ICA flow rates then this will increase confidence in the hypothesis that the link between the two is real and holds up over time.

It is highly likely that other factors not included in the previous models could play a role in predicting SCTLD incidence across scales within the Coral ECA. For example, coral disease can peak on reefs subjected to high levels of suspended sediment (Pollock et al. 2014) and chronic nutrient enrichment (Bruno et al. 2003), and where seasonal rainfall events result in episodic land-based runoff onto nearby coastal reefs (Haapkylä et al. 2011). The combination of outflow from ICAs in South Florida as well as land-based runoff following heavy rain events could result in raised nutrient and contaminant concentrations

of nearshore waters. Indeed, the previous temporal model (Walker et al. 2021a) still had 50.3% of the variation in SCTLD incidence unexplained and some of this could be explained by factors such as these. To address this, this current project includes the generation of a number of new predictor variables and their generation across novel scales. Specifically, the new temporal model includes monthly variations in **rainfall** that might drive additional land-based runoff and sedimentation to the reefs beyond the intentional release of waters from the ICAs. This project also includes additional metrics of coastal land use beyond septic tank densities as a proxy for urbanization in the new spatial model, specifically the **degree of coastal construction and impervious services** that promote land-based runoff.

Interestingly, despite previously identified links between water quality and coral disease dynamics in the literature, the previous models found no quantitative links between *in situ* water quality parameters and the occurrence of novel SCTLD lesions over space or time in the Coral ECA (Walker et al. 2021a). However, this could be due to the relatively poor temporal overlap between the response and predictor variables in the previous models. This current project includes a more robust exploration of the possible links between ICA flow rates and on-reef water quality, identifying whether any particular water quality parameter changes following periods of higher flow. This novel analysis builds on previous work (Whitall et al. 2019) and links the daily ICA flow rates to concurrent changes in a number of water quality parameters measured *in situ* (e.g. nitrate, nitrite, phosphorous) at the level of the reef benthos. Importantly, flow estimates were generated prior to the water quality sampling dates over several temporal windows. The goal was to identify the temporal window in historical flow rates that best explains any changes in water quality on the reef, potentially allowing the ability to infer travel times of water flow between the ICA inlets and the reef itself.

Finally, following advice from the DAC, this project also expanded the number of spatial scales over which septic tank densities were quantified in the spatial model and the number of temporal scales over which the flow rates from the ICAs were summarized in the temporal model. This allowed the scales that offer greatest predictive power to be identified, with the goal to improve the amount of variation the models explain. Importantly, if a particular scale offers more predictive power than another, then this may indicate something about how SCTLD incidence patterns and suspected drivers are linked and inspire future hypotheses for investigation.

3. Methods

Response variable data spatial processing

3.1 Disease incidence data

The response variable in this case is the number of novel SCTLD infections on several priority (n=69) large *O. faveolata* and *M. cavernosa* (n=37) corals that have been monitored by the project PI Brian Walker monthly from Sep 2018 to June 2021 (Figure 1). Each time a coral is visited, the number of SCTLD lesions are recorded. The lesions are then subsequently treated using techniques developed by the project team that are known to be successful (Walker and Brunelle 2018). This means that the number of SCTLD infections then recorded on each coral each month represents a measure of SCTLD incidence (novel development over time) (Figure 2). Such robust measures of coral disease incidence are rare highlighting the uniqueness and power of this dataset. Our monitored corals span a gradient of ~62 km from Key Biscayne to northern Broward County and cross numerous gradients in abiotic environmental conditions and local human impacts (Walker et al. 2021a).

Summary file: *LCDB_complete_aug2021_updated_PriorityCoralsOnly.csv*

Predictor variable data spatial processing

3.2 Coral host-specific variables

The previous analyses identified a negative correlation between the spatial variation in the total number of SCTLD infections and the proportion of live coral tissue on a colony remaining at the end of the disease monitoring timeseries (Walker et al. 2021a). To once again account for possible colony-specific attributes within the models, this synthesized information was updated. Specifically, colony-specific estimates of depth, planar length, planar width, planar height, linear length, linear width, colony total surface area, and the surface area of live tissue were quantified. After some consideration, however, the proportion of live coral tissue on a colony remaining at the end of the disease monitoring timeseries was not included in the updated spatial model presented here. SCTLD results in substantial tissue death and therefore the amount of live tissue at the end of the survey period could purely reflect the impact of the disease, rather than being a predictor (cause) of it.

Summary file: *LCDB_complete_aug2021_updated_PriorityCoralsOnly.csv*

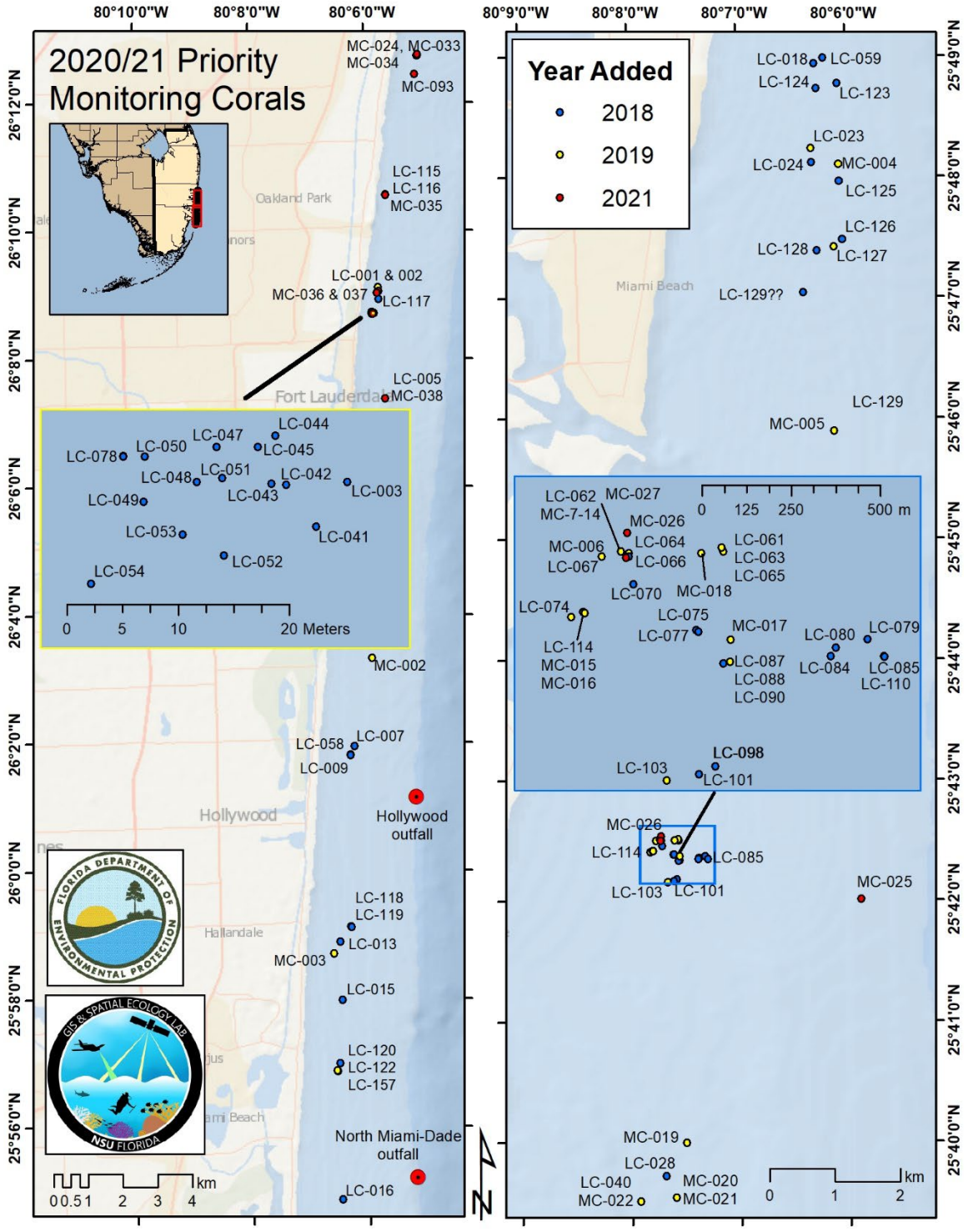

Figure 1. Location of the priority monitored corals within the Coral ECA.

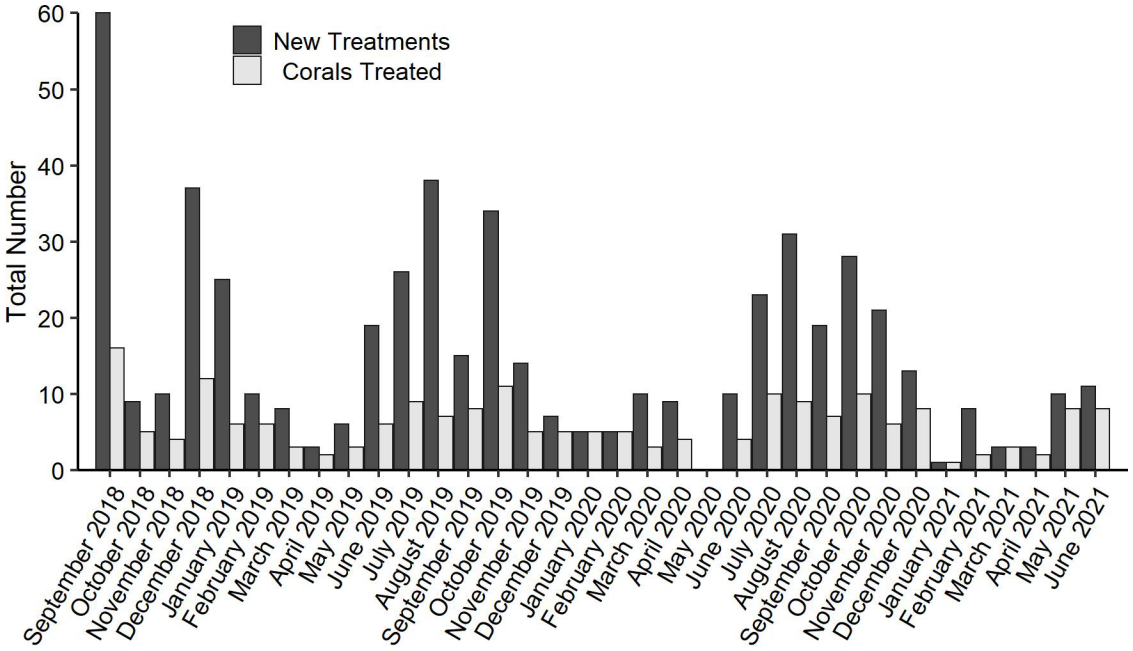

Figure 2. The total number of all new treatments and corals treated during each monitoring period within the Coral ECA.

3.3 *In situ* water temperature

Periods of extreme high temperatures have been linked to increased prevalence and incidence of coral diseases on reefs (Bruno et al. 2007; McClanahan et al. 2009; Williams et al. 2011). Temperature stress experienced by the monitored large corals was calculated using data from the long-term SECREMP monitoring programs.

The long-term SECREMP monitoring programs routinely deploys and retrieves HOBO© temperature loggers within the vicinity of the sampled/monitored corals and provided the full temporal coverage of the project survey period. Each large coral was spatially joined to the nearest logger. From the temperature timeseries, the seasonal mean and standard deviation for each summer period (July 1st – September 31st) was calculated. From this, the number of anomalously high temperature events was computed using the "Hot Snap" metric, defined as any temperature event that exceeds 1SD of the long-term seasonal mean (Heron et al. 2010). "Period of accumulation" was set to 3, 7, 30 and 90 days, meaning that for each monthly coral survey across the disease survey timeline, the number of Hot Snaps was calculated over these various temporal windows prior to the survey date. The summed number of Hot Snap events were multiplied by two to estimate the number of exposure hours over each temporal window (due to the 2-hr sampling resolution of the loggers, i.e., one event equals two hours, two events equal 4 hours and so on). Loggers were exposed to solar irradiance which may affect their readings, however they were consistently deployed between sites and should be accurate relative to each other (Bahr et al. 2016).

Summary file: *Hobo_Hotsnaps.csv*

3.4 *In situ* water quality

Increased nutrient concentrations and other water quality parameters like suspended solids can increase coral disease prevalence and severity within coral populations (Bruno et al. 2003; Voss and Richardson 2006; Pollock et al. 2014). This project utilized existing data from a long-term joint NOAA-FDEP water quality monitoring program across the Coral ECA in collaboration with Dr. David Whitall (National Centers for Coastal Ocean Science, NOAA) to quantify changes in water quality over time. The data represent monthly sampling at 71 sampling stations (Figure 3) to quantify a number of water quality parameters, of which the following analytes were focused on: 1) nitrate, 2) nitrite, 3) orthophosphate, 4) phosphorous, 5) total suspended solids, and 6) silicate.

The first task was to remove those sampling stations that were deliberately clustered around the inlets of each ICA (n=27) as these did not represent truly independent replicates of water quality (recorded in "*Inlet Nutrient sites to exclude.xlsx*"). This resulted in a total of 44 sampling stations included in all further analyses. The data were then filtered to focus on samples taken at the depth of the reef, not the surface.

The second task was to adjust the analyte values to account for the minimum detection limits (MDLs) of the two water quality processing labs (NOAA and GERG-Texas A&M). In the previous project, the MDL adjustments had already been completed by Dr David Whitall prior to supplying the data. Here however, the large extent of the data meant that it would have taken Dr. Whitall >6 months processing time to complete the calculations. This is partly due to the processing pipeline bottleneck of having to perform the calculations manually using a published Microsoft Excel-based methodology (Flynn 2010). As part of this project, a custom R routine (www.r-project.org) to re-create the Flynn (2010) methodology was created. The approach by Flynn maximizes the normality of a distribution of samples, after making a best-guess approach for values below a detection limit, set to half the reported detection limit for each analyte. Here, if an analyte had several different detection limits, the mean detection limit was used to approximate the best guess starting point for all values below the detection limit. Substantial QA/QC showed that this new R routine re-creates the output from Flynn (2010) exactly. The novel R routine developed under this project incorporates four existing R functions (*optim*, *readxl*, *dplyr*, *signal*) and combines these with a novel function (named "*shapiro_weights*") to calculate the Shapiro Weights used in Flynn (2010). The new routine consists of 170 lines of R code and is designed in such a way that the NOAA database files for the water quality monitoring program can be loaded directly into it with no need for any pre-processing. A user can therefore reproduce the Flynn (2010) methodology using the routine with minimal training and only a basic knowledge of R. The novel R routine significantly reduces the post-processing times for calculating the analyte MDLs, going from ~6 months person-time to a few days of auto-processing by a medium-spec computer (16 core, 30GB RAM).

Summary file: The synthesis of the water quality data for all 6 analytes across all 44 NOAA water quality sampling stations, representing monthly sampling from 2018 to 2021 formed a summary file of 14,994 rows: *Output_Corrected_Flynn_MDL_Data_by_Analyte.csv*.

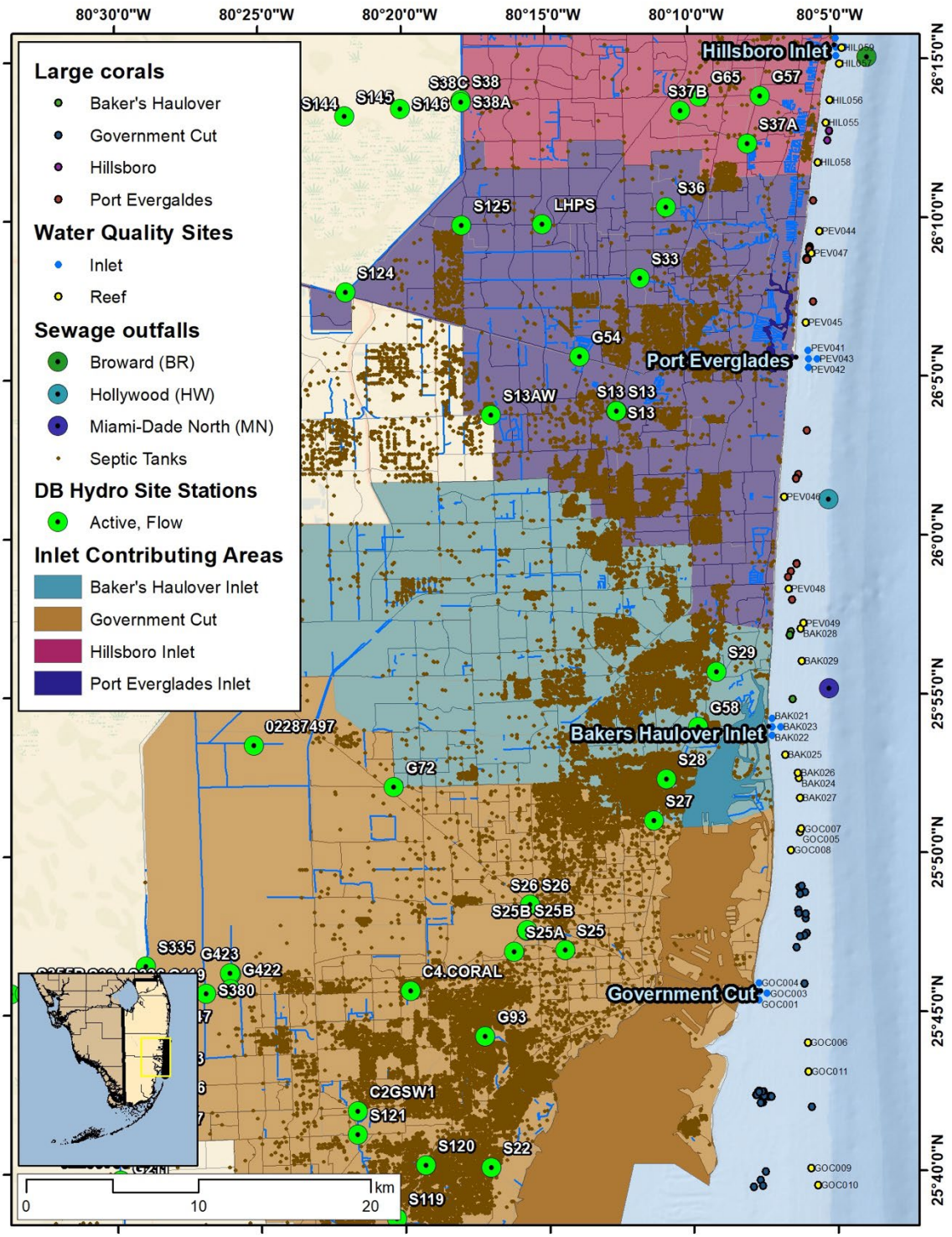

Figure 3. Location of all water quality monitoring sites and DBHydro monitoring site stations across the four ICAs. Also shown are the locations of the offshore sewage outfalls and the monitored large corals, the latter color coded by their respective ICAs.

The third task was to spatially join each of the monitored large corals to the NOAA water quality sampling stations to generate coral-specific estimates of the analyte concentrations the corals are exposed to over time. Each coral was joined to the five nearest five sampling stations using the *Generate Near Table* tool in ArcGIS, *sensu* Walker et al. (2021) and the distance (in m) of each coral to each of the water quality sampling stations was recorded. Then for each large coral survey date, concurrent water quality sampling events within a series of temporal windows were searched for (across their respective 1 or 5 sampling stations): 1, 3, 7, 14, 30, 60, and 90 days. The mean and standard deviation for each analyte was then computed. At the smaller temporal windows, this resulted in a large proportion of NA values in some cases.

Summary file: *Corals_Nutrients_5_Nearest.csv*

3.5 DBHydro flow data

The South Florida Water Management District's DBHydro monitoring stations (Figure 3) and database collects hydrologic, meteorologic, hydrogeologic and water quality data and is the source of historical and up-to-date environmental data for the 16-county region covered by the District. Using this database, estimates of water flow from individual ICAs to the monitored corals in the Coral ECA were used as a proxy for exposure to land-based sources of nutrients and pollutants. Unlike in the previous work (Walker et al. 2021a), here a sub-set of the DBHydro monitoring stations that independently captured the full extent of the flow within each ICA were identified. Stations that were upstream or downstream from each other, and therefore were artificially inflating summed flow values, were identified using a map of the flow channel paths throughout the ICAs and one of each pair removed. Through this iterative pairwise process, 20 stations were identified for inclusion in the analyses. Flow data for each ICA across the entire monitoring period of the large corals (2016-2021) were extracted, even prior to the identification of the "priority" corals used in our subsequent analyses. Flow patterns were relatively similar over time across the four ICAs, although temporal peaks in flow could be twice as high in Government Cut compared to the other ICAs (Figure 4). A pairwise correlation analysis showed that the similarity in temporal flow patterns varied between ICAs, with Baker's Haulover and Hillsboro the least correlated (r = 0.60), while Baker's Haulover & Government Cut and Hillsoboro & Port Everglades were the most highly correlated (r = 0.87) (Figure 5).

Summary file: *ICA_FLOW_DBHYDRO_icaname.csv*.

The next task was to spatially join the patterns in ICA flow to the monitored large corals. Each large coral was assigned to an ICA by identifying the nearest ICA inlet to it in space, regardless of direction north or south. The summed flow data for each coral from its respective ICA were then extracted over a series of temporal windows: 1, 3, 7, 14, 30, 60, and 90 days prior to each coral survey date.

Summary file: *ICA_Flow_Corals.csv*.

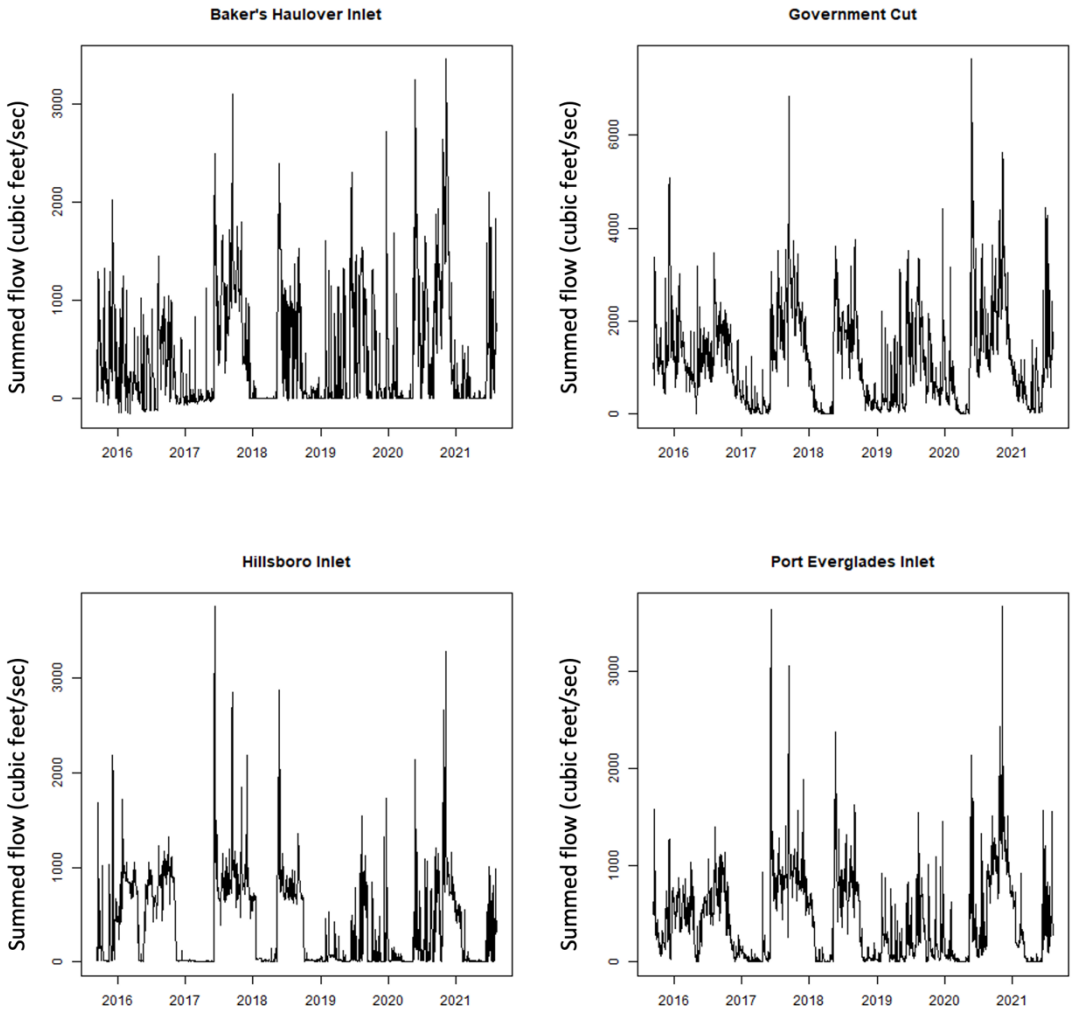

Figure 4. Temporal patterns in summed flow (in cubic feet per second) out of the ICA inlets over time.

3.6 Testing for relationships between ICA flow and water quality

Previous analyses by NOAA show there to be a correlation between *in situ* water nutrient concentrations and 'low' versus 'high' flow data from the DBHydro database (Whitall et al. 2019). This project builds on these analyses to treat the flow data as a continuous rather than a discrete (high versus low) predictor. Each water quality monitoring site was spatially joined to its closest ICA inlet using the *Closest Geodesic* option in ArcGIS Pro tool, *Spatial Join*. The summed flow data from the respective ICA over a series of temporal windows were then extracted: 1, 3, 7, 14, 30, 60, and 90 days prior to each sampling date at each water quality monitoring site. The data were summarized by analyte and by ICA.

Summary file: *ICA_Nutrients_Test.csv*.

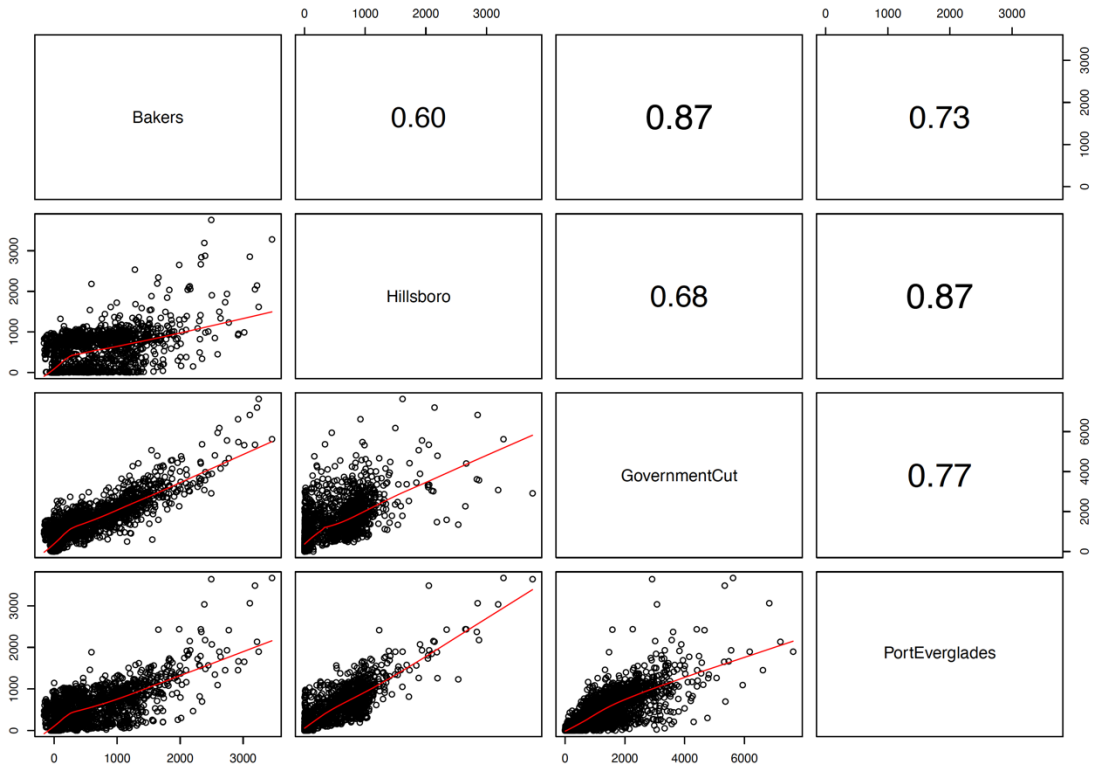

Figure 5. Pairwise Pearson's (*r*) correlations of the temporal patterns in summed flow (in cubic feet per second) out of the ICA inlets over time. The relationships have a smoothed regression line fitted (red line).

3.7 Timing of major sewer breaks.

Four datasets were obtained from the DEP Water Compliance Enforcement Program collected from the State Watch Office that contain data for spills in Broward and Miami-Dade County since 2000. The recording systems have changed over the years and the spreadsheets are different and contain varying degrees of different information. After evaluation, it was decided that these data were not useful in our statistical models.

3.8 Coastal land use

Land-based runoff to nearby coral reefs can be exacerbated by coastal urbanization that creates large expanses of impervious surfaces, such as concrete (Fabricius 2005; Brodie et al. 2012). This, in combination with high rainfall, can lead to high levels of nutrient runoff, poor water quality and sediment deposition that can promote coral disease establishment and persistence (Aeby et al. 2010; Haapkylä et al. 2011). This project utilized the NOAA Coastal Change Analysis Program (C-CAP) regional Land Cover and Change Dataset, a 30 x 30 m resolution satellite-based product that contains information on a variety of land uses across the Florida region (https://coast.noaa.gov/digitalcoast/data/ccapregional.html). The dataset was last updated in 2016 and the focus here was on estimating coastal

construction and development that could contribute to coastal runoff and pollution that might in turn trigger and exacerbate coral disease development. As such, two of the classes pertaining to Developed Land, namely Developed High Intensity and Developed Medium Intensity were synthesized. Developed High Intensity contains significant land area and is covered by concrete, asphalt, and other constructed materials. Vegetation, if present, occupies less than 20 % of the landscape. Constructed materials account for 80 – 100 % of the total cover. This class includes heavily built-up urban centers and large constructed surfaces in suburban and rural areas with a variety of land uses. Developed Medium Intensity contains areas with a mixture of constructed materials and vegetation or other cover. Constructed materials account for 50 – 79 % of total area. This class commonly includes multi- and single-family housing areas, especially in suburban neighborhoods, but may include all types of land use. The amount (in m^2) of Developed High Intensity and Developed Medium Intensity land within the vicinity of the monitored corals was quantified using a Fibonacci sequence of expanding radial buffers (1, 2, 3, 5, 8, 13, and 21 km).

Summary file: *Priority_Corals_Land_Cover.csv*

3.9 Rainfall patterns

Episodes of heavy rainfall can lead to land-based runoff to nearby coastal areas and contribute to the establishment and persistence of coral diseases (Haapkylä et al. 2011). Furthermore, such events can stir up deposited sediment and introduce new sediment sources from the land into suspension that can also exacerbate coral disease (Pollock et al. 2014). This project utilized the South Florida Water Management District's Daily Historical Rainfall database (www.sfwmd.gov/weather-radar/rainfall-historical/daily) to quantify the mean daily rainfall experienced prior to each disease survey over several temporal windows. A total of 33 stations that fell within the bounds of the four ICAs were selected (these can be found in the summary file "Rainfall_Stations.csv") and daily rainfall values computed across the entire disease survey timeseries for each individual ICA.

Summary file: *ICA_RAIN_DBHYDRO_ icaname.csv*

3.10 Human population density

Previous works have shown a link between local human impacts and coral disease prevalence, specifically using local human population density as a proxy for cumulative impacts (Aeby et al. 2011b). To quantify human populations within the vicinity of the coral disease survey locations this project used the 2019 U.S. Census Population and Housing Unit Counts dataset for Florida (https://www.census.gov/geographies/mapping-files/time-series/geo/tiger-data.html). Specifically, the project used the geodatabase entitled "ACS_2019_5YR_BG_12.gdb". Using R, this was joined with the Census table X01_AGE_AND_SEX, using the two columns: B01001e1 and B01001m1, that is defined by the metadata table: SEX BY AGE: Total: Total population -- (Estimate).

Summary file: *Priority_Corals_Human_Population_Density.csv*

3.11 Distance to outfall locations and septic tanks

The pairwise linear distances (in m) of each surveyed large coral to each sewage outfall location (BAK030, PEV050, HIL060, BOC080, GOC014) was calculated (Figure 3).

Summary file: *DISTANCE_TO_ALL_OUTFLOWS_Priority_Corals.csv*

The number of septic tanks within the vicinity of each coral was quantified using the expanding radial buffers (1, 2, 3, 5, 8, 13, and 21 km) using data from the 'Our Florida Reefs' online database (https://ourfloridareefs.org) for the year 2013.

Summary file: *Data_Output/Count_Septic_Tanks_Buffers_Corals.csv*

3.12 GIS data

For each of the data layers described above, any relevant ArcGIS files, R code files, and data output files have been archived at NSU and provided to FDEP. These are organized into folders named by the predictor variable of interest (Tasks 2.1 to 2.12).

3.13 ArcGIS geodatabase

For each of the completed data layers described above (Tasks 2.1 to 2.12), an ArcGIS geodatabase summary has been built containing all relevant primary and meta-data for each predictor variable georeferenced over all the defined spatial and temporal scales. These are archived at NSU and have been provided to FDEP.

3.14 Statistical modeling

Modeling the links between ICA flow and on-reef water quality

This analysis utilized 6132 individual water quality analyte measurements from 2018 to 2010. Initial data exploration showed that examining flow over the previous 3 days prior to water sample collections would yield the strongest relationships. The possible links between ICA inlet flow and changes in the water quality parameters (nitrate, nitrite, phosphorous, orthophosphate, silicate, total suspended solids) were modeled using generalized additive models (GAMs) (Wood 2006a) with the *mgcv* package for R (Wood 2012). The analyte response variables were logged and fitted to the flow values to allow for random smooths by ICA and year (penalized deviations from the main smooth), using restricted maximum likelihood (REML) as follows:

gam(log(X) ~ s(flow, bs=c("tp")) + te(flow, ICA, year, bs=c("tp","re","re"))

where “tp” represents a thin-plate regression spline (an isotopic smoother term) (Wood 2003) and “re” represents a parametric term penalized by a ridge penalty (Wood 2006b). This approach allowed a global trend to be modeled, as well identifying whether and in what ways individual ICAs or years diverged substantial from this trend.

SCTLD incidence modeling

Coral disease data are challenging to model due to the often zero-inflated nature of the data resulting from low overall disease prevalence and incidence within coral populations (Williams et al. 2010; Aeby et al. 2011a; Aeby et al. 2011b). This means many traditional statistical modeling techniques are inappropriate. Here pattern of SCTLD incidence were modeled using distance-based permutational multiple regression (McArdle and Anderson 2001). The approach carries out a partitioning of variation in a data set described by a resemblance matrix according to a multiple regression model. Predictor variables can be categorical or continuous and the technique makes no prior assumptions about the nature of the response variable distribution, meaning that normality does not have to be satisfied. The power of this monitoring data set is to be able to say with confidence whether corals experienced repeat infections over the time period and if they did, to what degree and what might be driving this variation.

To models patterns in SCTLD incidence over time (temporal model), the unit of replication was ‘survey month’. The goal was to maximize temporal replication (survey months) while minimizing spatial bias. Across the various monitored large corals, the start of the timeseries was set to September 2018, when the maximum number of large corals (n=68) all began to be routinely monitored; the timeseries then ran until June 2021. To contribute to the temporal model, the large corals had to be susceptible to SCTLD (i.e., had at least 1 lesion recorded across the entire timeseries from Sep 2015 to Aug 2021) and been surveyed in at least 32 out of the 34 survey months, resulting in 47 large corals being included (Appendix 1). For each survey month, the total number of novel lesions was summed across these 47 corals and then related over time to concurrent changes in the predictor variables.

To models patterns in SCTLD incidence over space (spatial model), the unit of replication were the individual large corals themselves. The goal was to maximize spatial replication (number of colonies) while minimizing temporal bias. The start of the timeseries was set to July 2019, when the maximum number of corals were surveyed. Of these 90 corals, 66 showed susceptibilities to SCTLD (i.e., had at least 1 lesion recorded across the entire timeseries from Sep 2015 to Aug 2021) and were included in the spatial modeling process (Appendix 2). For each coral, the total number of novel lesions was summed across the 24-month period and then related to concurrent spatial changes in the predictor variables.

Prior to model fitting, the predictor variables (n=21 temporal model, n=39 spatial model) were investigated for collinearity by calculating pairwise Pearson’s correlations (*r*). For

any that equaled $r > 0.8$, one of the two predictors were removed. Which variable was removed was based on the suspected ability to interpret the mechanistic link between the predictor and response variable should the predictor variable emerge as important, as well as attempting to ensure spread across the various spatial/temporal scales computed for each predictor. This resulted in a total of 12 and 17 predictor variables included in the temporal and spatial model fitting process, respectively (Appendix 3, 4). The predictors were normalized to account for variations in their data range and units and all possible candidate models (unique combinations of the predictors) were computed. These were then ranked based on Akaike Information Criterion (Akaike 1973) with a second-order bias correction applied (AICc) (Hurvich and Tsai 1989; Burnham and Anderson 2004) to account for the relatively large number of predictor variables relative to independent response variables. After fitting the distance-based permutational multiple regression models, the significant predictors explaining temporal and spatial variations in SCTLD were investigated in more detail for possible non-linear effects on disease dynamics using generalized additive models (GAM).

4. RESULTS

4.1 Links between ICA flow and on-reef water quality

There were significant relationships between ICA inlet flow over the previous 3 days and the on-reef concentration of all six water quality analytes (Table 1). Model performance ranged from 22.7 to 40.6% deviance explained, and there were significant effects of total flow on nitrate and nitrite after accounting for the effects of ICA and year (Table 1). The patterns between flow and the remaining four analytes (orthophosphate, phosphorus, silicate and total suspended solids) were purely driven by individual effects within certain ICAs and years (Table 1, Appendix 5).

Most of the relationships identified were positive, such that increases in flow resulted in an increased concentration of the analyte. For example, as flow increased, the concentration of both nitrate and nitrite increased, up until a certain summed flow when the concentrations started to level off (Figure 6). This suggests that initial increases in flow result in marked increases in on-reef nitrate and nitrite, but that there then comes a saturation point, particularly for nitrite concentration above ~5000 cubic feet/second summed flow (Figure 6). For nitrate, some ICAs had more pronounced patterns than others, particularly in certain years. For example, in 2018 there were clear positive trends between flow and on-reef nitrate concentration in Baker's Haulover and Hillsboro, but not Government Cut or Port Everglades Inlet; in some years, however, these positive trends appeared to break down (Figure 7). Similarly for nitrite, some ICAs again had more pronounced patterns than others, particularly in certain years. In 2018, for example, there was a clear positive trend in Baker's Haulover more so than in the other ICAs (Figure 8). The relationships between flow and orthophosphate, phosphorus, silicate and total suspended solids can be found in Appendix 5. These patterns would benefit from further investigation, in particular building a model to test how flow might interact and combine with rainfall patterns to drive on-reef water quality.

Table 1. Generalized additive model (GAM) results testing for a relationship between ICA inlet flow over the previous 3 days and concentration of six on-reef water quality analytes.

Analyte	Smooth terms	P value	Deviance explained (%)
Nitrate	s(flow)	**0.0188**	
	te(flow, ICA, year)	**<0.0001**	22.7
Nitrite	s(flow)	**0.0259**	
	te(flow, ICA, year)	**<0.0001**	39.2
Orthophosphate	s(flow)	0.377	
	te(flow, ICA, year)	**<0.0001**	40.6
Phosphorus	s(flow)	0.331	
	te(flow, ICA, year)	**<0.0001**	25.2
Silicate	s(flow)	0.102	
	te(flow, ICA, year)	**<0.0001**	24.4
TSS	s(flow)	0.953	
	te(flow, ICA, year)	**<0.0001**	10.7

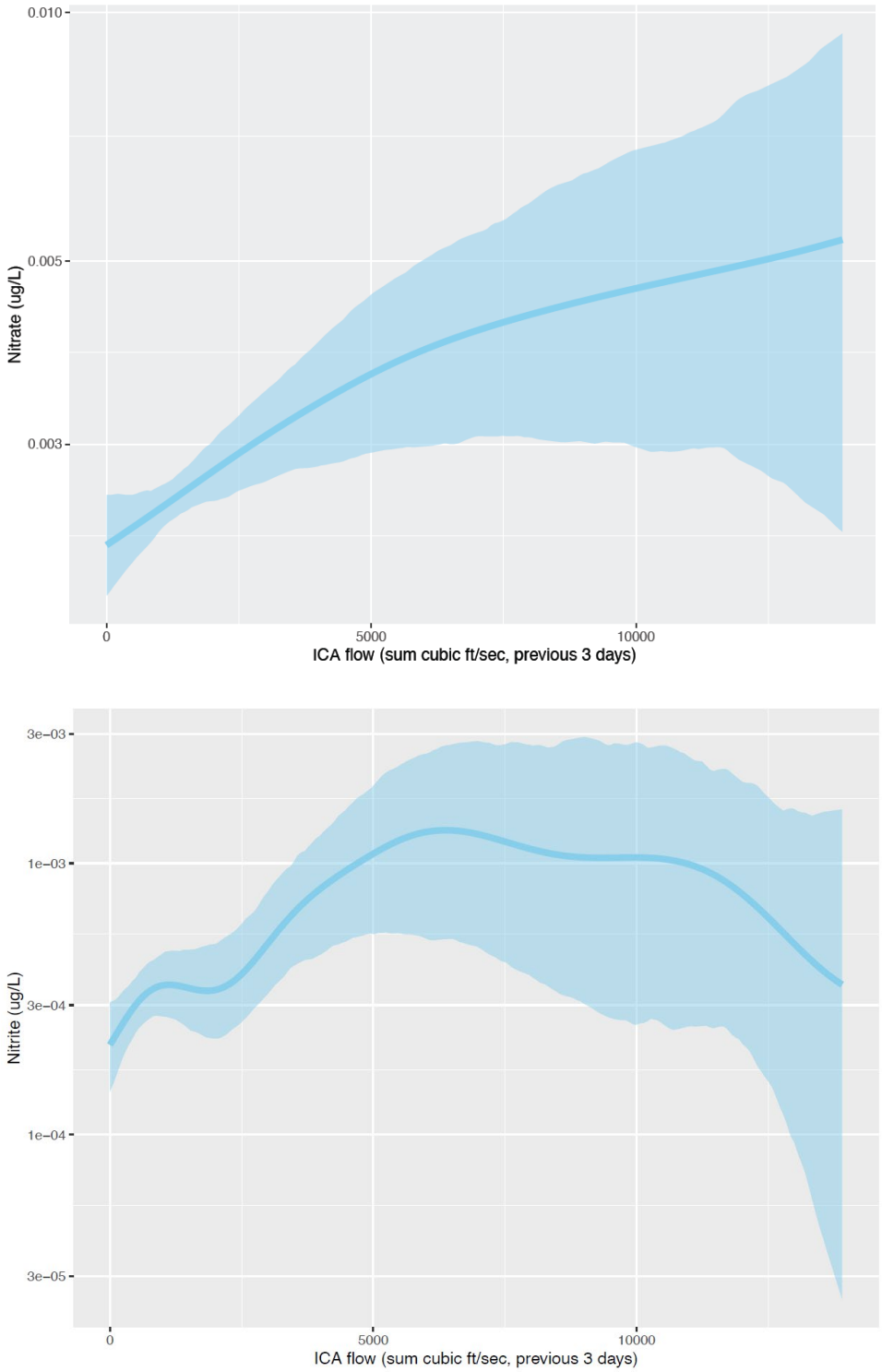

Figure 6. Global effect of ICA inlet flow over the previous 3 days and concentration of on-reef nitrate (top) and nitrite (bottom), having accounted for variations across individual ICAs and years. Solid line represents the model fit and shading represents the 95% confidence interval.

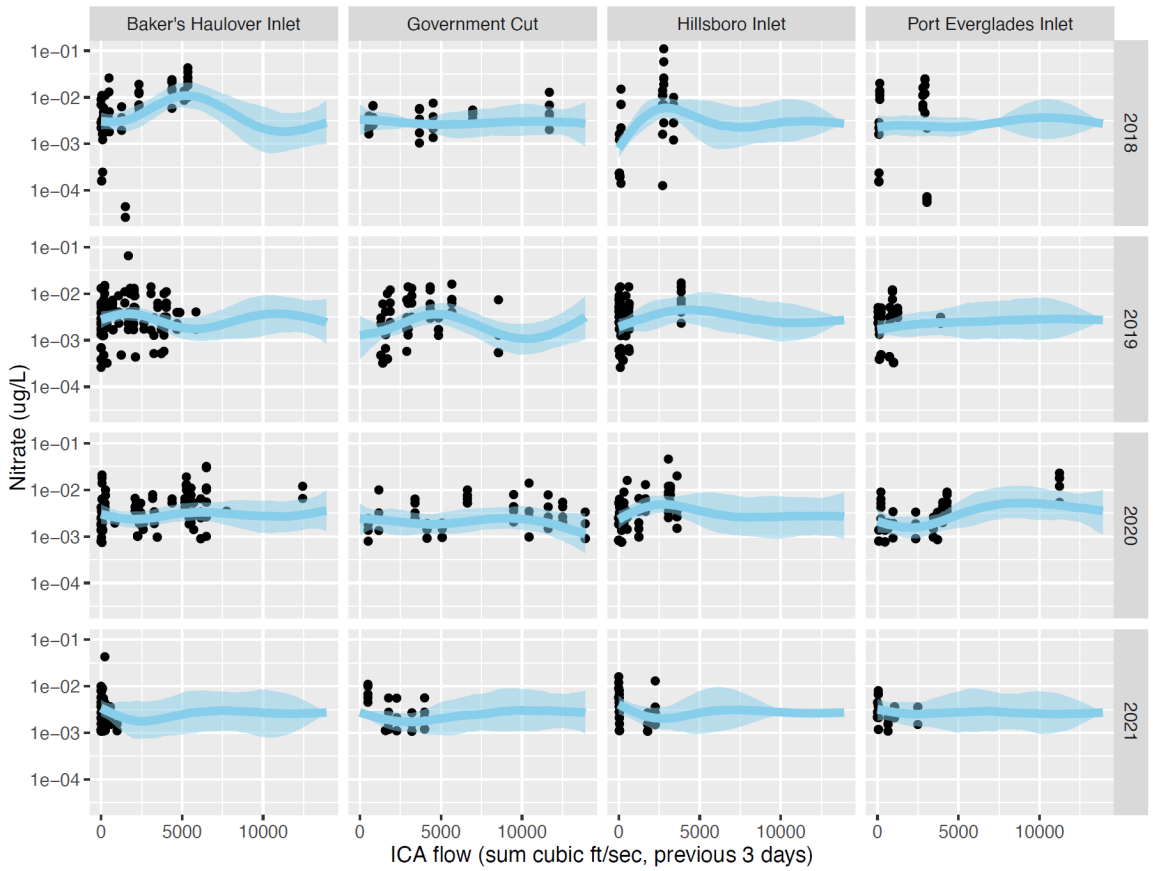

Figure 7. Relationship between ICA inlet flow over the previous 3 days and concentration of on-reef **nitrate** across individual ICAs and years. Solid line represents the model fit and shading represents the 95% confidence interval. The black circles indicate the underlying data in each case. Where no data exists, the fits represent model predictions based on trends in other ICAs/years that inform the smoother terms in these regions.

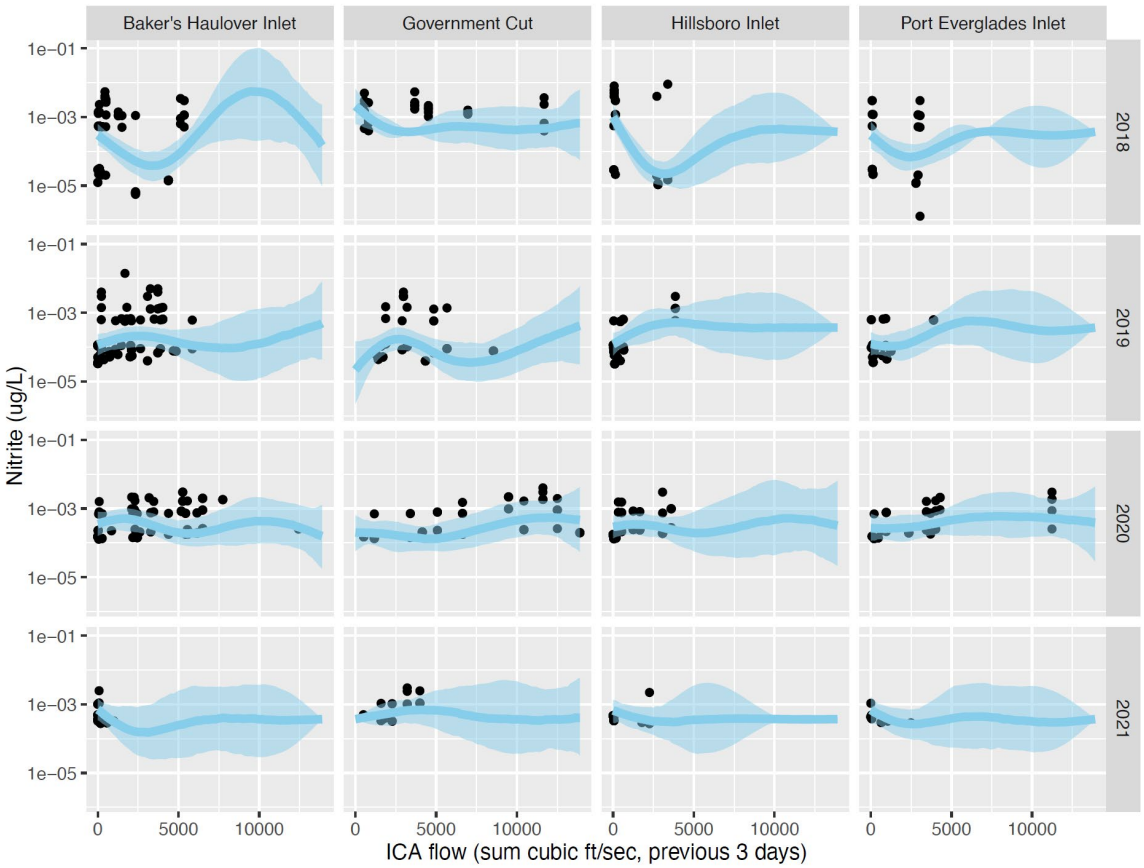

Figure 8. Relationship between ICA inlet flow over the previous 3 days and concentration of on-reef **nitrite** across individual ICAs and years. Solid line represents the model fit and shading represents the 95% confidence interval. The black circles indicate the underlying data in each case. Where no data exists, the fits represent model predictions based on trends in other ICAs/years that inform the smoother terms in these regions.

4.2 Drivers of temporal and spatial patterns in SCTLD incidence

Temporal model: The total number of novel SCTLD lesions (disease incidence) varied over time and ranged from 0 to 60 in any given month from September 2018 to June 2021 (Figure 9). There was only one survey month (May 2020) when zero lesions were recorded. This temporal variation was best explained by a model containing three predictors (Table 2), namely exposure to temperature stress ('Hot Snaps') in the 90 days prior (35.6% variation explained), flow out of the ICA inlets over the previous 7 days (14.1% variation explained), and mean daily rainfall in the 90 days prior (6.7% variation explained). Overall, this model explained 56.4% of the temporal variation in the total number of SCTLD infections over time (Table 2).

SCTLD infections showed a positive correlation with temperature stress (Figure 10), a positive correlation with inlet flow (Figure 11), and a positive correlation with total rainfall (Figure 12). Outliers created high model error for both temperature stress and inlet flow towards the higher values of both predictors (Appendix 6). It appears more SCTLD lesions develop over time following a pro-longed period of temperature stress, in particular when there has been over 150 'Hot Snap' exposure hours over the prior 90 days. This is then exacerbated by higher outflow from the ICA inlets and heavier rainfall, in particular when there has been more than 5000 cubic feet per second summed flow coming out of the ICAs in the prior 7 days, and more than 0.2 – 0.3 inches of rain per day over the prior 90 days. However, flow over the previous 7 days collineated highly with flow over the previous 14 and 30 days (14 and 30 days were therefore excluded from our model fitting process, Appendix 3), and so any of these temporal windows would likely offer similar predictive power. A more cautious interpretation, therefore, would be that flow over the previous 7 to 30 days shows a positive relationship with SCTLD lesion development over time.

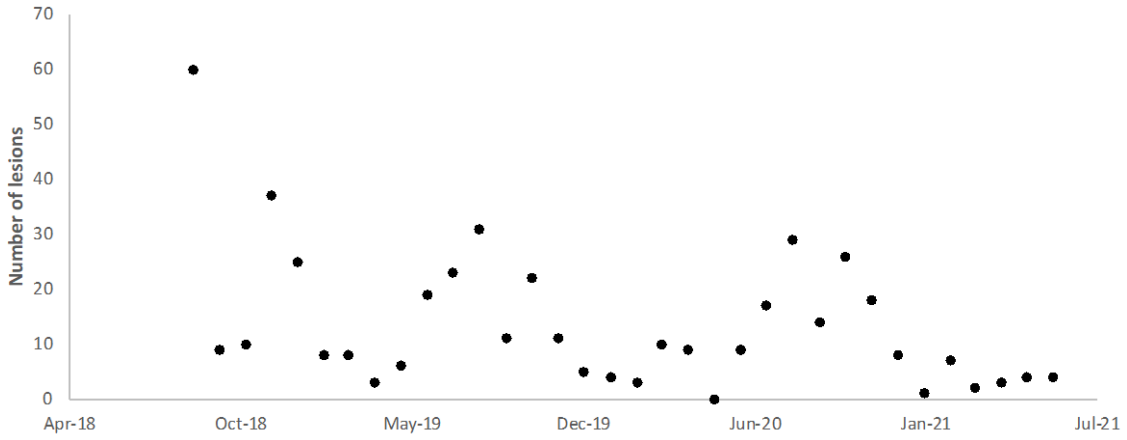

Figure 9. SCTLD disease incidence (number of novel SCTLD lesions over time) on 52 large corals monitored monthly from September 2018 to June 2021.

Table 2. Temporal and spatial model summaries, showing statistics for the predictors included in the optimal models, the percentage of variation in the response variable they explain (Prop) and their cumulative percentage of variation they explain (Cumul).

	Predictor	SS(trace)	Pseudo-F	P	Prop (%)	Cumul (%)
Temporal Model	HotSnap (90 days)	1814.0	17.14	0.001	35.6	35.6
	Flow (7 days)	717.4	5.08	0.027	14.1	49.7
	Mean Rain (90 days)	343.7	2.24	0.042	6.7	56.4
Spatial Model	Septic (5 km)	1649.4	21.75	0.001	25.4	25.4
	Government Cut (distance km)	816.8	12.75	0.001	12.6	38.0

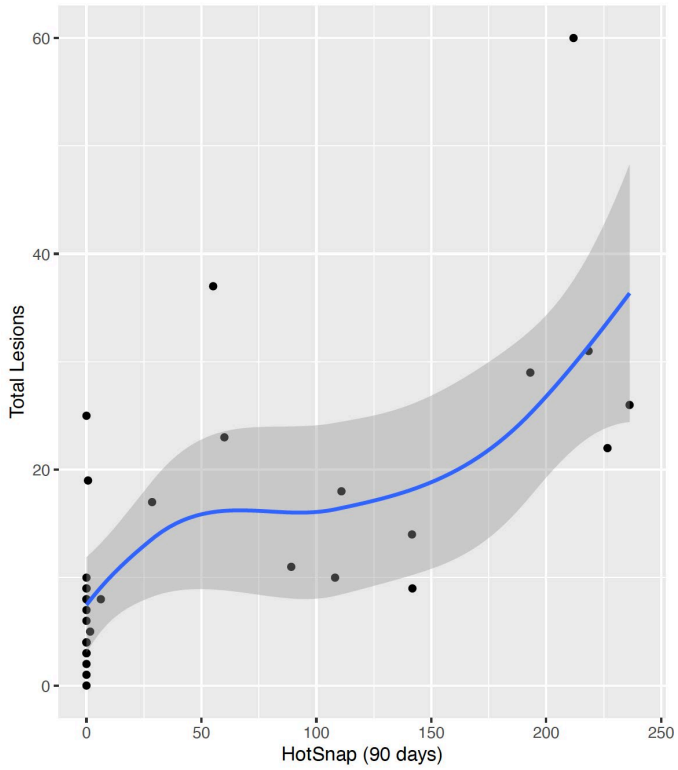

Figure 10. Relationship between seawater temperature stress (total 'Hot Snap' exposure hours) over the prior 90 days and number of novel SCTLD lesions developing over time. Note the x-axis is trimmed to emphasize the relationship and exclude the high model error after Hot Snap >250 (n=1 data point).

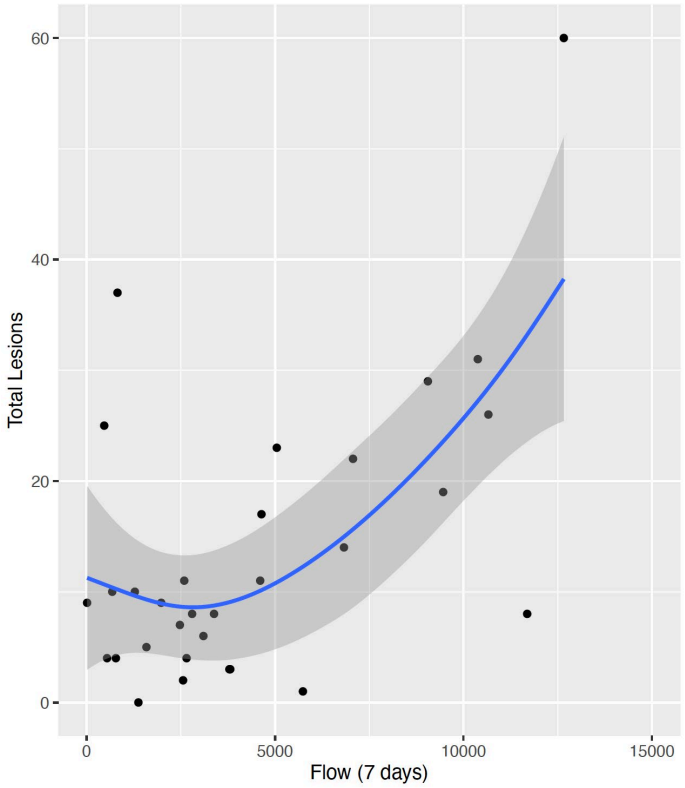

Figure 11. Relationship between ICA inlet flow (summed cubic feet per second) over the prior 7 days and number of novel SCTLD lesions developing over time. Note the x-axis is trimmed to emphasize the relationship and exclude the high model error after flow >15000 (n=2 data points).

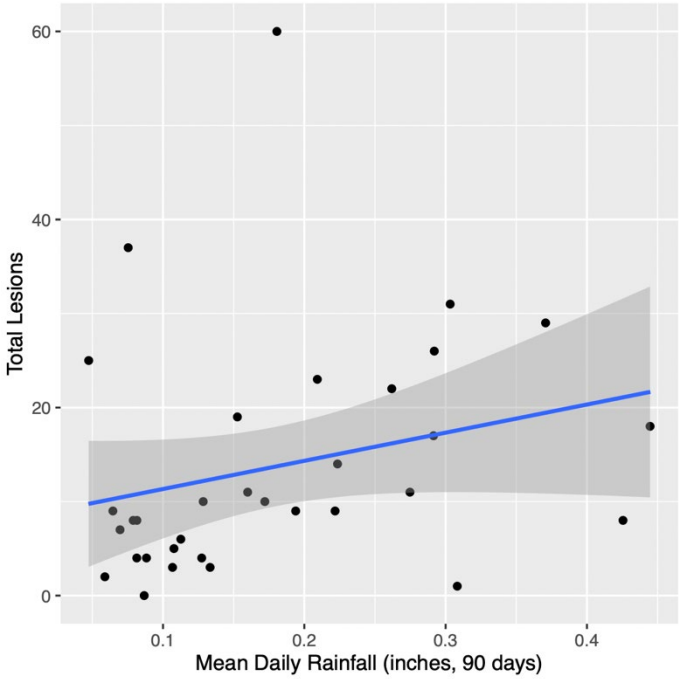

Figure 12. Relationship between mean daily rainfall (in inches) over the prior 90 days and number of novel SCTLD lesions developing over time.

Spatial model: The total number of SCTLD infections ranged from 0 to 44 on any individual large coral colony from July 2019 to June 2021. This spatial variation was best explained by a model containing two predictors (Table 2), namely the number of septic tanks within a 2 km radius (25.4% variation explained) and the linear distance to the Government Cut outfall (12.6% variation explained). Overall, this model explained 38.0% of the spatial variation in the total number of SCTLD infections over the entire period (Table 2).

SCTLD infections showed a positive correlation with the number of septic tanks within a 5 km radius, with a noticeable increase in lesions occurring beyond ~100 tanks (Figure 13). The correlation with the distance to the Government Cut outfall was less clear, with the number of lesions maximized at mid-distances (Figure 14). This should be interpreted with caution, however, as the distance to Government Cut outfall highly correlated with the distance to both Hillsboro and Boca outfalls, suggesting that either of these distances might offer the same predictive power in the model.

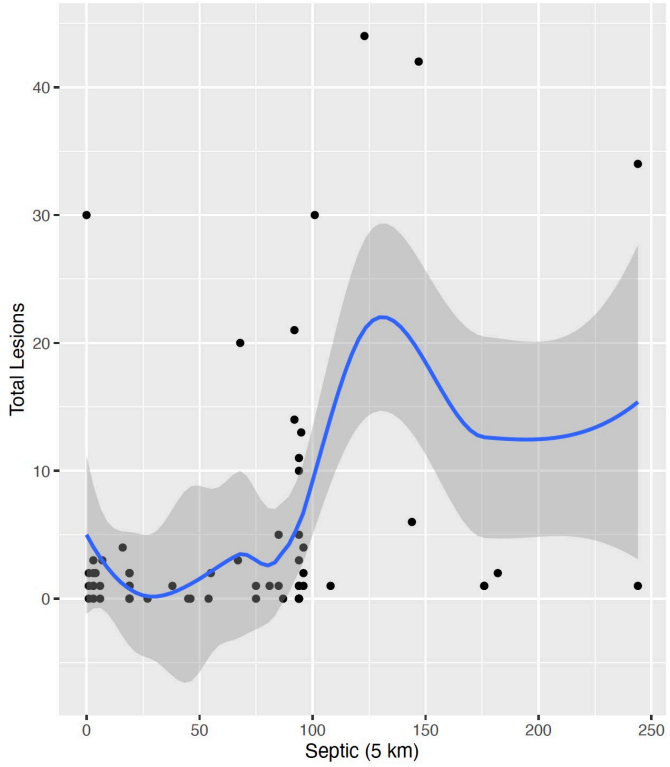

Figure 13. Relationship between the number of septic tanks within a 5 km radius and spatial variations in the total number of novel SCTLD lesions.

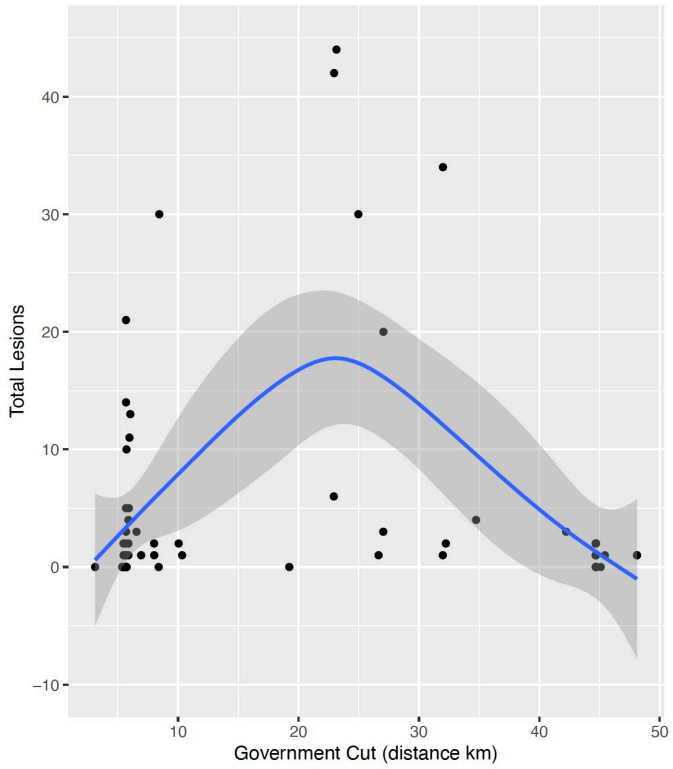

Figure 14. Relationship between the linear distance (in km) to Government Cut outfall and spatial variations in the total number of novel SCTLD lesions.

Sensitivity analyses

The Ft. Lauderdale cluster of corals potentially introduces spatial autocorrelation that might invalidate the statistical assumptions of data independence in the spatial model (Walker et al. 2021b). The spatial model was therefore re-run with all but one of these corals removed (LC-047) to see what effect this has on the model results. Overall, the results were very similar. The optimal model still contained the same two predictors and explained 37.8% of the spatial variation in the total number of SCTLD infections over the entire period. Given that this represented a reduction of 0.2% variation explained compared to the model presented in Table 2, it is concluded that the effect of the Ft. Lauderdale cluster of corals are minimal to non-existent.

5. CONCLUSIONS AND FUTURE WORK

This project identified a correlation between: 1) on-reef nutrient concentrations (water quality) and ICA inlet flow; 2) inlet flow and SCTLD incidence in the Kristin Jacobs Coral Reef Ecosystem Conservation Area (Coral ECA); and, 3) SCTLD incidence and exposure to stress caused by anomalously high seawater temperatures associated with global warming. The sum consequence of these relationships we have identified is that global stressors on corals are being exacerbated by the local human impacts of runoff and land-based sources of pollution that elevate on-reef nutrient levels. Mitigating local stressors

would make conditions for corals less conducive to disease. These links highlight that there are management, conservation, and stewardship actions in SE Florida that can increase reef resilience to climate change and disease outbreaks. As one example, the timing of inlet outflow can be regulated to ensure high flow does not coincide with periods of high seawater temperature stress. Future work can help to shape and target this and a range of other actions to maximize our influence on the capacity of reefs in SE Florida to function and provide goods and services under climate change.

Previous attempts to identify direct links between SCTLD patterns and in situ on-reef nutrient concentrations were unsuccessful. The disease surveys and water quality sampling have taken place in different locations and at different times (Walker et al. 2021a). Future efforts must focus on overcoming this data mis-match by generating more spatially resolute water quality data using spatial interpolation. These maps would provide water quality estimates for all locations within the Coral ECA. Even though there would be varying levels of confidence in the interpolated data, this approach would allow a more direct comparison of water quality and SCTLD incidence. We can then determine the broader influence of water quality on coral and reef fish communities within the Coral ECA. We are now positioned to lead collaborative projects to deliver on this proposed research and help to target and shape actions that support reef resilience.

Acknowledgements. We thank Andrew Davies (University of Rhode Island) and Dieter Tracey (Science Graphics/SymbioSeas) for help with the development of the predictor variable data layers used in our analyses, and Tim Jackson Bué (Bangor University) for advice on approaches for quantifying spatial autocorrelation.

References

Aeby GS, Ross M, Williams GJ, Lewis TD, Work TM (2010) Disease dynamics of *Montipora* white syndrome within Kaneohe Bay, Oahu, Hawaii: distribution, seasonality, virulence, and transmissibility. Dis Aquat Org 91:1-8

Aeby GS, Williams GJ, Franklin EC, Kenyon J, Cox EF, Coles S, Work TM (2011a) Patterns of Coral Disease across the Hawaiian Archipelago: Relating Disease to Environment. PloS One 6:e20370

Aeby GS, Howells E, Work T, Abrego D, Williams GJ, Wedding LM, Caldwell JM, Moritsch M, Burt JA (2020) Localized outbreaks of coral disease on Arabian reefs are linked to extreme temperatures and environmental stressors. Coral Reefs 39:829-846

Aeby GS, Williams GJ, Franklin E, Haapkyla J, Harvell CD, Neale S, Page CA, Raymundo L, Vargas-Angel B, Willis B, Work TM, Davy SK (2011b) Growth anomalies on the coral genera *Acropora* and *Porites* are strongly associated with host density and human population size across the Indo-Pacific. PLoS One 6:e16887

Akaike H (1973) Information theory as an extension of the maximum likelihood principal, pp. 261-281 in Petrov BN and Caski F (eds). Proceedings, 2nd International Symposium on Information Theory. Akademiai Kiado, Budapest.

Alvarez-Filip L, Estrada-Saldívar N, Pérez-Cervantes E, Molina-Hernández A, González-Barrios FJ (2019) A rapid spread of the stony coral tissue loss disease outbreak in the Mexican Caribbean. PeerJ 7:e8069

Bahr, K. D., Jokiel, P. L., & Rodgers, K. U. S. (2016). Influence of solar irradiance on underwater temperature recorded by temperature loggers on coral reefs. *Limnology and Oceanography: Methods*, *14*(5), 338-342.

Brodie J, Kroon F, Schaffelke B, Wolanski E, Lewis S, Devlin M, Bohnet I, Bainbridge Z, Waterhouse J, Davis A (2012) Terrestrial pollutant runoff to the Great Barrier Reef: An update of issues, priorities and management responses. Mar Pollut Bull 65:81-100

Bruno JF, Petes LE, Harvell CD, Hettinger A (2003) Nutrient enrichment can increase the severity of coral diseases. Ecol Lett 6:1056-1061

Bruno JF, Selig ER, Casey KS, Page CA, Willis BL, Harvell CD, Sweatman H, Melendy AM (2007) Thermal stress and coral cover as drivers of coral disease outbreaks. PLoS Biol 5:1220-1227

Burnham KP, Anderson DR (2004) Multimodel inference - understanding AIC and BIC in model selection. Social Method Res 33:261-304

Estrada-Saldívar N, Quiroga-García BA, Pérez-Cervantes E, Rivera-Garibay OO, Alvarez-Filip L (2021) Effects of the Stony Coral Tissue Loss Disease Outbreak on Coral Communities and the Benthic Composition of Cozumel Reefs. Frontiers in Marine Science 8:306

Fabricius KE (2005) Effects of terrestrial runoff on the ecology of corals and coral reefs: review and synthesis. Mar Pollut Bull 50:125-146

Flynn MR (2010) Analysis of censored exposure data by constrained maximization of the Shapiro–Wilk W statistic. The Annals of Occupational Hygiene 54:263-271

Haapkylä J, Unsworth RK, Flavell M, Bourne DG, Schaffelke B, Willis BL (2011) Seasonal rainfall and runoff promote coral disease on an inshore reef. PLoS One 6:e16893

Heron SF, Willis BL, Skirving WJ, Eakin CM, Page CA, Miller IR (2010) Summer Hot Snaps and Winter Conditions: Modelling White Syndrome Outbreaks on Great Barrier Reef Corals. PloS One 5:e12210

Hurvich CM, Tsai CL (1989) Regression and time-series model selection in small samples. Biometrika 76:297-307

Maynard J, van Hooidonk R, Eakin CM, Puotinen M, Garren M, Williams G, Heron SF, Lamb J, Weil E, Willis B, Harvell CD (2015) Projections of climate conditions that increase coral disease susceptibility and pathogen abundance and virulence. Nature Clim Change 5:688-694

McArdle BH, Anderson MJ (2001) Fitting multivariate models to community data: A comment on distance-based redundancy analysis. Ecology 82:290-297

McClanahan TR, Weil E, Maina J (2009) Strong relationship between coral bleaching and growth anomalies in massive *Porites*. Global Change Biol 15:1804-1816

Muller EM, Sartor C, Alcaraz NI, van Woesik R (2020) Spatial Epidemiology of the Stony-Coral-Tissue-Loss Disease in Florida. Frontiers in Marine Science 7:163

Pollock FJ, Lamb JB, Field SN, Heron SF, Schaffelke B, Shedrawi G, Bourne DG, Willis BL (2014) Sediment and turbidity associated with offshore dredging increase coral disease prevalence on nearby reefs. PloS one 9:e102498

Voss JD, Richardson LL (2006) Nutrient enrichment enhances black band disease progression in corals. Coral Reefs 25:569-576

Walker BK, Brunelle A (2018) Southeast Florida large (>2 m) diseased coral colony intervention summary report. Florida DEP & FWC. Miami, FL. Pp. 1-164.

Walker BK, Williams GJ, Maynard JA (2021a) 2020-2021 Coral ECA Reef-building-coral Disease Intervention, Statistical Modelling, and Preparation for Restoration Task 6 Final Report: Environmental drivers of stony coral tissue loss disease. Florida DEP. Miami, FL. 120p.

Walker BK, Williams GJ, Aeby GS, Maynard JA, Whitall D (2021b) Environmental and human drivers of stony coral tissue loss disease (SCTLD) incidence within the Southeast Florida Coral Reef Ecosystem Conservation Area, 2021-22. 1st Interim Progress Report. Florida DEP. Miami, FL., 19 p.

Whitall D, Brickner S, Cox D, Baez J, Stamates J, Gregg K, Pagan F (2019) Southeast Florida Reef Tract Water Quality Assessment. NOAA Technical Memoradum NOS NCCOS 271. Silver Spring. 116 pages.

Williams GJ, Aeby GS, Cowie ROM, Davy SK (2010) Predictive Modeling of Coral Disease Distribution within a Reef System. PLoS One 5:e9264

Williams GJ, Knapp IS, Work TM, Conklin EJ (2011) Outbreak of *Acropora* white syndrome following a mild bleaching event at Palmyra Atoll, Northern Line Islands, Central Pacific. Coral Reefs 30:621

Wood SN (2003) Thin plate regression splines. J Roy Stat Soc Ser B (Stat Method) 65:95-114

Wood SN (2006a) Generalized additive models: an introduction with R. CRC Press

Wood SN (2006b) Low-Rank Scale-Invariant Tensor Product Smooths for Generalized Additive Mixed Models. Biometrics 62:1025-1036

Wood SN (2012) mgcv: GAMs with GCV/AIC/REML smoothness estimation and GAMMs by PQL. R package.version 1.7-22

Appendices

Appendix 1. Monitored large corals included in the temporal model (Sep-18 to Jun-21) (n=47). Those shaded grey satisfied the temporal replication requirements but have never shown susceptibility to SCTLD since monitoring began and so were excluded from the analysis.

LC-002	LC-043	LC-066	LC-114
LC-003	LC-044	LC-070	LC-115
LC-005	LC-047	LC-075	LC-116
LC-007	LC-048	LC-077	LC-118
LC-009	LC-049	LC-078	LC-119
LC-013	LC-050	LC-079	LC-120
LC-015	LC-051	LC-080	LC-122
LC-016	LC-052	LC-085	LC-123
LC-018	LC-053	LC-090	LC-124
LC-024	LC-054	LC-098	LC-126
LC-028	LC-058	LC-101	LC-127
LC-041	LC-059	LC-103	LC-128
LC-042	LC-062	LC-110	LC-129

Appendix 2. Monitored large corals included in the spatial model (n=66).

LC-002	LC-047	LC-067	LC-115	MC-004
LC-003	LC-048	LC-070	LC-116	MC-005
LC-005	LC-049	LC-074	LC-117	MC-006
LC-007	LC-050	LC-075	LC-118	MC-007
LC-009	LC-051	LC-077	LC-119	MC-008
LC-013	LC-052	LC-078	LC-120	MC-009
LC-015	LC-053	LC-079	LC-122	MC-010
LC-016	LC-054	LC-080	LC-123	MC-011
LC-018	LC-055	LC-084	LC-124	MC-013
LC-023	LC-056	LC-085	LC-125	MC-014
LC-024	LC-058	LC-087	LC-126	MC-015
LC-028	LC-059	LC-088	LC-127	MC-016
LC-040	LC-061	LC-090	LC-128	MC-017
LC-041	LC-062	LC-098	LC-129	MC-018
LC-042	LC-063	LC-101	LC-157	MC-019
LC-043	LC-064	LC-103	MC-001	MC-020
LC-044	LC-065	LC-110	MC-002	MC-021
LC-045	LC-066	LC-114	MC-003	MC-022

Appendix 3. Predictor variables included in the temporal model fitting process.

1	Flow_1	Exclude
2	Flow_3	Exclude
3	Flow_7	Trial
4	Flow_14	Exclude
5	Flow_30	Exclude
6	Flow_60	Trial
7	Flow_90	Trial
8	Rain_1	Exclude
9	Rain_3	Trial
10	Rain_7	Trial
11	Rain_14	Trial
12	Rain_30	Exclude
13	Rain_60	Trial
14	Rain_90	Trial
15	HotSnap_1	Exclude
16	HotSnap_3	Trial
17	HotSnap_7	Trial
18	HotSnap_14	Exclude
19	HotSnap_30	Trial
20	HotSnap_60	Exclude
21	HotSnap_90	Trial

Appendix 4. Predictor variables included in the spatial model fitting process.

1	depth_ft	Trial
2	length_planar	Exclude
3	width_planar	Trial
4	height_planar	Trial
5	length_linear	Trial
6	width_linear	Trial
7	landuse_medium_1km	Exclude
8	landuse_high_1km	Trial
9	landuse_medium_2km	Exclude
10	landuse_high_2km	Exclude
11	landuse_medium_3km	Exclude
12	landuse_high_3km	Exclude
13	landuse_medium_5km	Exclude
14	landuse_high_5km	Exclude
15	landuse_medium_8km	Exclude
16	landuse_high_8km	Exclude
17	landuse_medium_13km	Exclude
18	landuse_high_13km	Trial
19	landuse_medium_21km	Exclude
20	landuse_high_21km	Trial
21	HumPop_1km	Trial
22	HumPop_2km	Trial
23	HumPop_3km	Exclude
24	HumPop_5km	Exclude
25	HumPop_8km	Exclude
26	HumPop_13km	Exclude
27	HumPop_21km	Trial
28	Septic_1km	Exclude
29	Septic_2km	Trial

30	Septic_3km	Exclude
31	Septic_5km	Trial
32	Septic_8km	Exclude
33	Septic_13km	Exclude
34	Septic_21km	Trial
35	Bakers_Haulover	Trial
36	Boca	Exclude
37	Government_Cut	Trial
38	Hillsboro	Exclude
39	Port_Everglades	Trial

Appendix 5. Relationship between ICA inlet flow over the previous 3 days and concentration of on-reef orthophosphate, phosphorus, silicate and total suspended solids (TSS) across individual ICAs and years. Solid line represents the model fit and shading represents the 95% confidence interval. The black circles indicate the underlying data in each case. Where no data exists, the fits represent model predictions based on trends in other ICAs/years that inform the smoother terms in these regions.

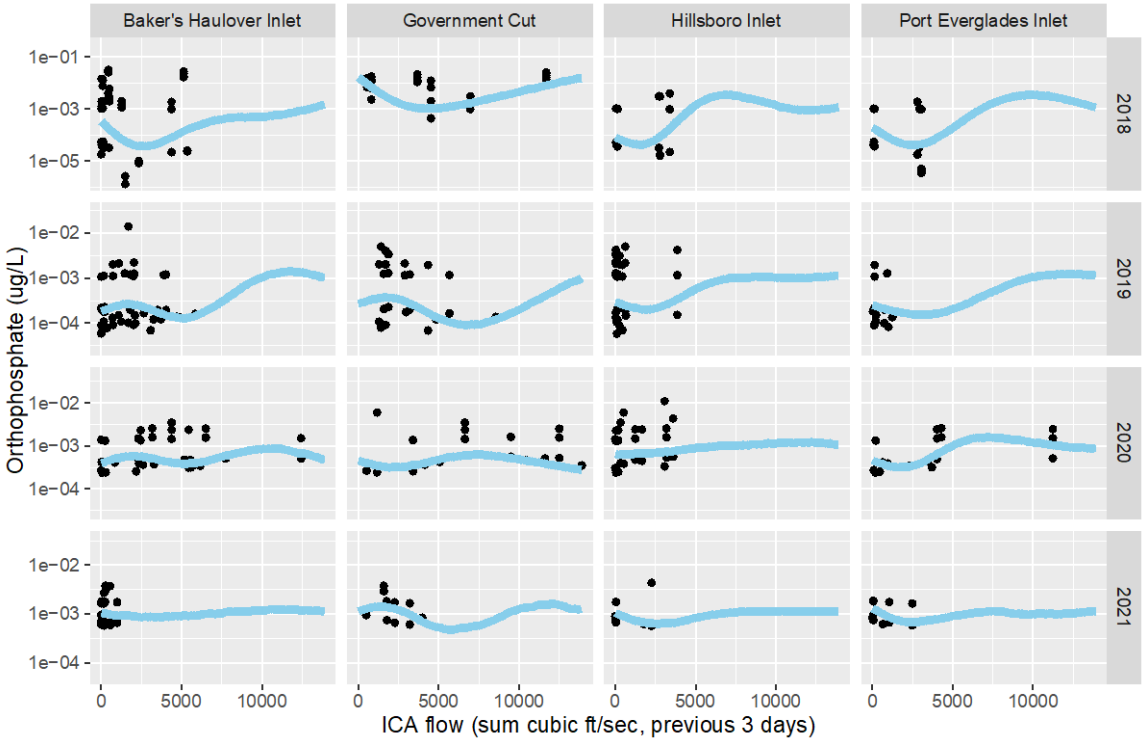

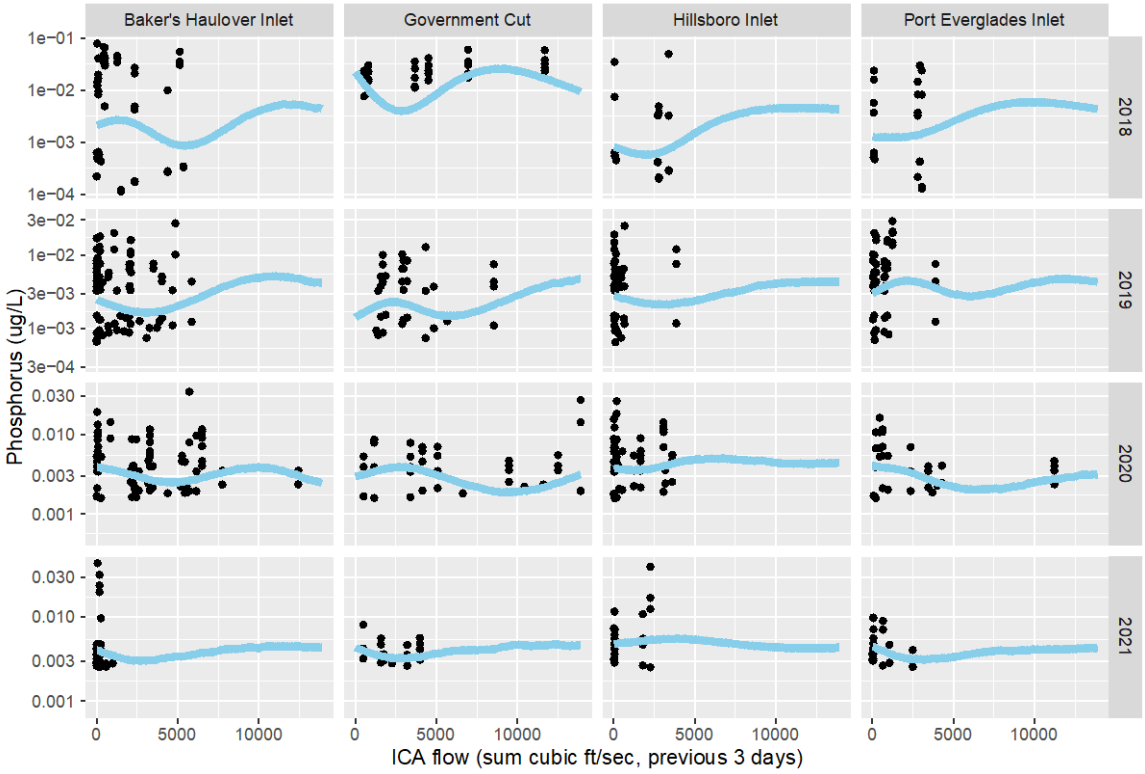
Baker's Haulover Inlet
Government Cut
Hillsboro Inlet
Port Everglades Inlet
2018
2019
2020
2021
Phosphorus (ug/L)
1e−01
1e−02
1e−03
1e−04
3e−02
3e−03
3e−04
0.030
0.010
0.003
0.001
0
5000
10000
ICA flow (sum cubic ft/sec, previous 3 days)

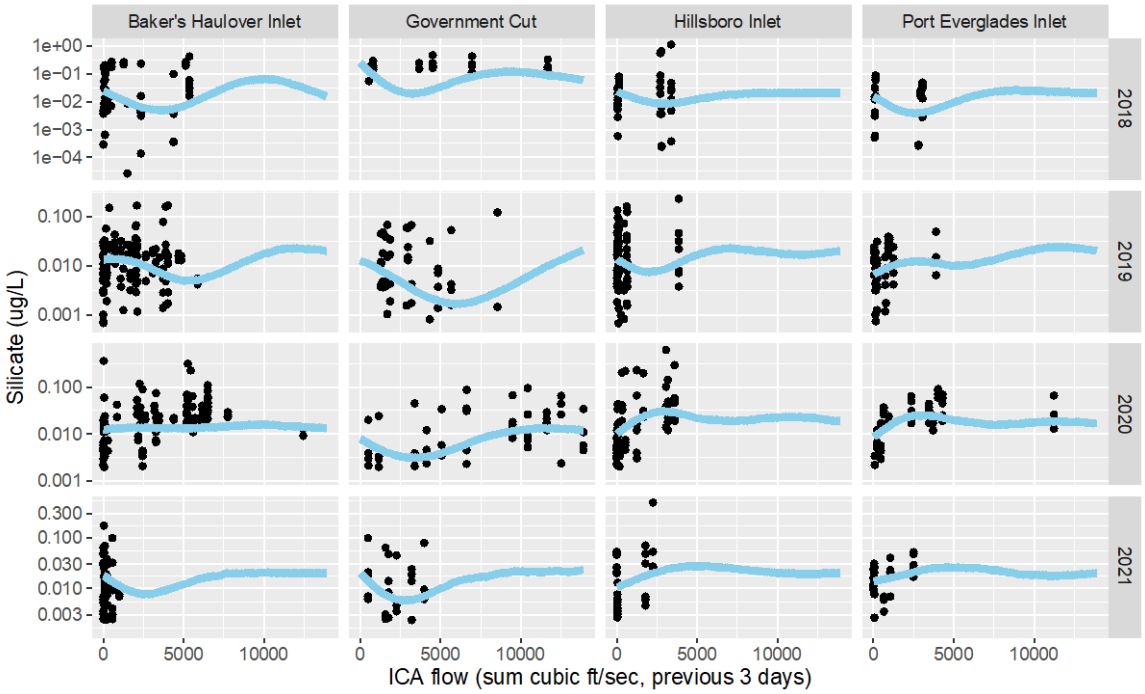
Baker's Haulover Inlet
Government Cut
Hillsboro Inlet
Port Everglades Inlet
2018
2019
2020
2021
Silicate (ug/L)
1e+00
1e−01
1e−02
1e−03
1e−04
0.100
0.010
0.001
0.300
0.030
0.003
0
5000
10000
ICA flow (sum cubic ft/sec, previous 3 days)

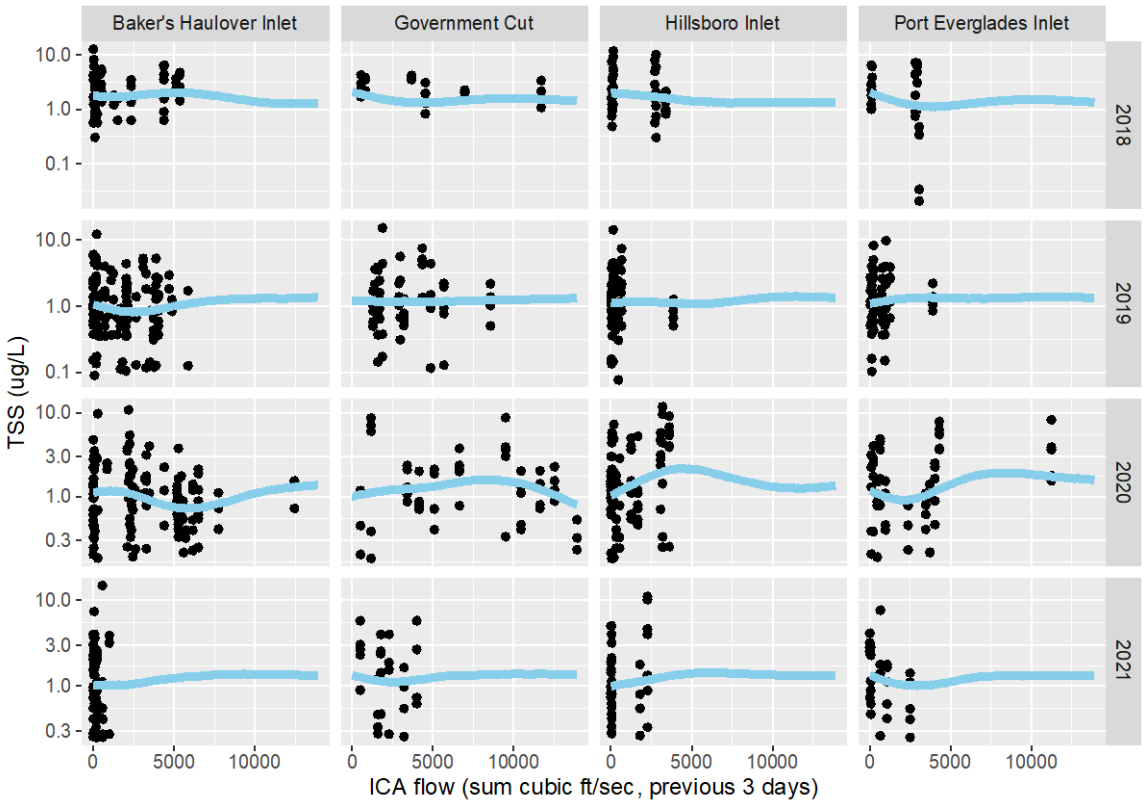

Appendix 6. Relationship between seawater temperature stress (total 'Hot Snap' exposure hours) over the prior 90 days and number of novel SCTLD lesions developing over time, and the relationship between inlet flow stress over the prior 7 days and number of novel SCTLD lesions developing over time – both with the complete x-axis model error displayed.